

## Direct Formation of Solution-based Al<sub>2</sub>O<sub>3</sub> on Epitaxial Graphene Surface for Sensor Applications

Kwan-Soo Kim,\* Hirokazu Fukidome, and Maki Suemitsu

Research Institute of Electrical Communication (RIEC), Tohoku University,  
2-1-1 Katahira, Aoba-ku, Sendai, Miyagi 980-8577, Japan

(Received January 31, 2019; accepted February 25, 2019)

**Keywords:** epitaxial graphene, solution process, sensor, microwave annealing

We propose a method for fabricating high-performance epitaxial graphene field-effect transistors (EG-FETs), involving a microwave-annealing-treated solution-based Al<sub>2</sub>O<sub>3</sub> (MWA-treated sol-Al<sub>2</sub>O<sub>3</sub>) layer as a gate dielectric. The MWA process substantially preserves the pristine properties of EG with minimal hole doping and strain induction. The MWA-treated sol-Al<sub>2</sub>O<sub>3</sub> showed a surface roughness of ~0.33 nm, a dielectric constant of 7.5, and a leakage current of  $8.7 \times 10^{-6}$  A/cm<sup>2</sup>. The transconductance of the MWA-based EG-FET presents an enhanced field effect mobility by a factor of about 8 compared with the EG-FET with a natural oxide of Al.

### 1. Introduction

Graphene is a promising material for sensing applications owing to its extremely high carrier mobility, exceptional surface-to-volume ratio, and low contact resistance. Among various graphene formation methods, that of epitaxial graphene (EG) proceeds via the sublimation of Si atoms from the surface of SiC substrates and provides a practical technology in that it enables a uniform formation of monolayer graphene over a large area and requires no transferring process onto insulating substrates for the fabrication of devices.<sup>(1–3)</sup>

An ion-sensitive field-effect transistor (IS-FET) is a representative electrochemical sensor device that converts a chemical signal into an electrical signal.<sup>(4,5)</sup> In the IS-FET, the formation of a high-quality gate oxide is essential for obtaining a high sensitivity. The epitaxial graphene field-effect transistor (EG-FET) is no exception. One of the challenges in EG-based sensor fabrication, however, is to establish a reliable process for gate dielectric formation that overcomes such difficulties as the hydrophobic nature of graphene,<sup>(6)</sup> induced damage during plasma processing,<sup>(7)</sup> and the onset of strain and doping during the high-temperature annealing process.<sup>(8)</sup> In this respect, the choice of the right dielectric material and a damage-free deposition technique for that material are the keys to the realization of EG-based sensor applications.

The solution-based (sol–gel) process is attractive in that gate dielectrics with a simple, low-temperature, low-cost, defect-free, and large-area-compatible process can be fabricated.<sup>(9,10)</sup>

\*Corresponding author: e-mail: kimks@riec.tohoku.ac.jp

<https://doi.org/10.18494/SAM.2019.2317>

In this process, thermal annealing at temperatures above 400 °C is required to eliminate the solvent and absorb the moisture from air to oxidize the metal precursor. When applied to graphene, however, this high temperature treatment can cause unwanted hole doping and strain. In order to overcome these limitations, we have succeeded in forming high-quality solution-based Al<sub>2</sub>O<sub>3</sub> on EG grown on Si-face SiC by introducing the microwave annealing (MWA) process. Because of the dielectric heating of the substrate, MWA generates heat from inside of the substrate. This unique heating property allows extremely high heating efficiencies, ramp rates, and in-plane uniformities,<sup>(11,12)</sup> which contribute to the minimization of the annealing time and the suppression of the generation of hole doping in graphene.

In this study, we investigated how MWA improved the electrical properties of EG-FETs with solution-based Al<sub>2</sub>O<sub>3</sub> gate dielectrics. The dielectric properties were evaluated by fabricating a capacitor. As the unique properties of MWA, we found that the MWA-treated sol-Al<sub>2</sub>O<sub>3</sub> shows a high dielectric constant, a low leakage current, and a small surface roughness without the generation of defects, doping, or strain in graphene. Moreover, we found that the formation of a high-quality gate dielectric contributed greatly to the improvement of transconductance and the reduction of the subthreshold swing of EG-FETs.

## 2. Materials and Methods

### 2.1 Direct formation of sol-Al<sub>2</sub>O<sub>3</sub> on EG surface

Epitaxial graphene was grown on a p-type doped (resistivity >  $1.0 \times 10^9 \Omega\text{cm}$ ), C-face 6H-SiC(000-1) substrate (II-VI Inc). After chemical cleaning, we graphitized its surface under Ar atmosphere at 1420 °C for 5 min. The Al<sub>2</sub>O<sub>3</sub> precursor solution was prepared by dissolving aluminum isopropoxide (Kojundo Chemical Laboratory) in xylene together with a stabilizer solution and a thinner solution (Al<sub>2</sub>O<sub>3</sub> precursor:thinner = 1:1). The formation process of the sol-Al<sub>2</sub>O<sub>3</sub> layer is similar to the photoresist coating process. After spin coating of the prepared solution, the sample was immediately baked with a hot plate at 120 °C for 2 min. To remove organics and residual chemicals in the film, O<sub>2</sub> plasma treatment at 30 W for 2 min was subsequently conducted.<sup>(13)</sup> MWA was conducted using a conventional microwave oven with a fixed frequency of 2.45 GHz under the output powers of 500 and 1000 W. Microwave irradiation was conducted for 1 min and repeated several times with at least a 5 min interval in between. Under this condition, the temperature of the sample easily rises to 500 °C within 1 min at 1000 W [Fig. 1(a)]. The heating ability of MWA is mainly determined by the dielectric loss of the material, the efficiency to convert electromagnetic energy into thermal energy.<sup>(14,15)</sup> The dielectric loss of SiC increases with the doping concentration,<sup>(16)</sup> and it is actually possible to achieve temperatures at and above 1700 °C by using highly doped 4H-SiC substrates implanted with Al<sup>+</sup> and P<sup>+</sup> ions.<sup>(17)</sup> In this study, however, the need for the use of a highly resistive SiC substrate for EG-FET fabrication limits the maximum achievable temperature at 600 °C. This temperature is still sufficiently high as we will see later. We also prepared two reference samples: one with a natural oxide layer of Al (~3 nm) and the other with a sol-Al<sub>2</sub>O<sub>3</sub> layer fabricated by conventional postdeposition annealing (PDA) at 250 °C for 2 h. The

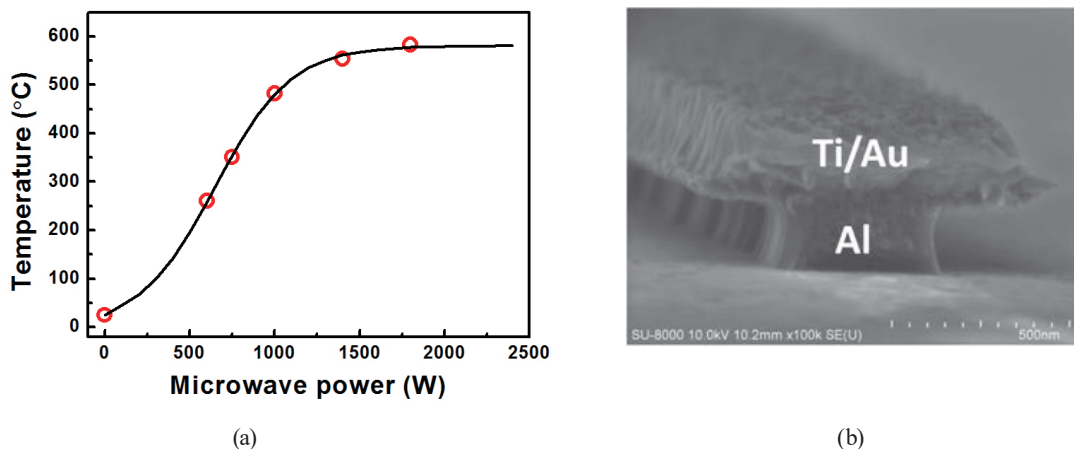


Fig. 1. (Color online) (a) Temperature of the SiC substrate as a function of the microwave irradiation power applied for 1 min. (b) SEM image of the T-shaped metal gate formed by a selective metal undercut technique.

damage, doping, and strain of the EG before and after sol-Al<sub>2</sub>O<sub>3</sub> formation were characterized by Raman scattering spectroscopy ( $\lambda = 514$  nm). The surface roughness and the chemical composition of the sol-Al<sub>2</sub>O<sub>3</sub> layer were characterized by atomic force microscopy (AFM) and X-ray photoelectron spectroscopy (XPS), respectively.

## 2.2 Fabrication of metal-oxide-semiconductor (MOS) capacitor and EG-FETs

To evaluate the electrical characteristics of Al<sub>2</sub>O<sub>3</sub> films, we fabricated MOS capacitors on n-type (100) Si wafers with an e-beam-evaporated Ti/Au (5 nm/50 nm) layer as a metal electrode. We also fabricated self-aligned EG-FETs using a T-shaped metal gate. After the patterning of the channel region and the source/drain region, the T-shaped metal gate was fabricated by a selective metal undercut technique. First, a stack of a thin sol-Al<sub>2</sub>O<sub>3</sub> layer and a thick Al film was formed on the substrate. The thicknesses of the sol-Al<sub>2</sub>O<sub>3</sub> and Al metal were 10 and 150 nm, respectively. After patterning the gate region (gate length = 1  $\mu$ m) by EB lithography, a Ti/Au (10 nm/150 nm) gate metal was deposited using an EB evaporator. Finally, the stack of sol-Al<sub>2</sub>O<sub>3</sub> and Al layers was selectively etched using boiling phosphoric acid at 100 °C. The Ti/Au metal acted as a hard mask during the wet etching, and the sol-Al<sub>2</sub>O<sub>3</sub>/Al layer underneath the Ti/Au was selectively etched. Figure 1(b) shows the SEM image of the T-shaped metal gate structure formed by the selective metal undercut technique. The access length is about 300 nm and the gate length and the access length can be controlled by adjusting the etching time. The electrical characteristics of these MOS capacitors were obtained with a semiconductor parameter analyzer (Agilent B1500).

### 3. Results and Discussion

#### 3.1 Raman spectrum of EG before and after MWA

First, the damage caused by MWA on the EG properties was examined by Raman scattering spectroscopy. Figure 2(a) shows the Raman spectra of EG grown on C-face SiC under various MWA conditions. Under all MWA conditions, the EG essentially preserves its pristine qualities as evidenced by the absence of the defect-related D-bands at around  $1350\text{ cm}^{-1}$ . This indicates that the present microwave irradiation causes no significant damage in graphene.

The Raman spectrum also provides important information on the doping and strain of EG in its G- and G'-band positions.<sup>(18)</sup> Figures 2(b) and 2(c) show the histograms of the G- and G'-band positions, respectively. The orange line in Fig. 2(b) corresponds to the sol-Al<sub>2</sub>O<sub>3</sub> film formed by PDA on EG. A substantial blue shift is observed in this case in the G-band position while the G'-band position does not change. This indicates the onset of hole doping, which can be ascribed to the insufficient decomposition and elimination of the C-, O- and H-bearing fragments in the film as well as to the subsequent oxygen penetration into EG. In sharp contrast, no such doping is observed for EG capped with MWA-treated Al<sub>2</sub>O<sub>3</sub> films. This suppression is understood to be due to our controlled use of MWA in this experiment. SiC is known to be one of the most efficient microwave absorbers ever tested,<sup>(19)</sup> and the temperature of the MWA-heated SiC can easily rise to  $\sim 600\text{ }^{\circ}\text{C}$  in a few minutes.

#### 3.2 Surface morphology of MWA-treated sol-Al<sub>2</sub>O<sub>3</sub>

The surface roughness is also a key parameter that determines the carrier scattering and carrier mobility in EG-FETs. Figure 3 shows the AFM images of (a) EG on C-face SiC, (b) the natural oxide layer of Al, and (c) the sol-Al<sub>2</sub>O<sub>3</sub> layer fabricated by iterations of 1 min MWA at

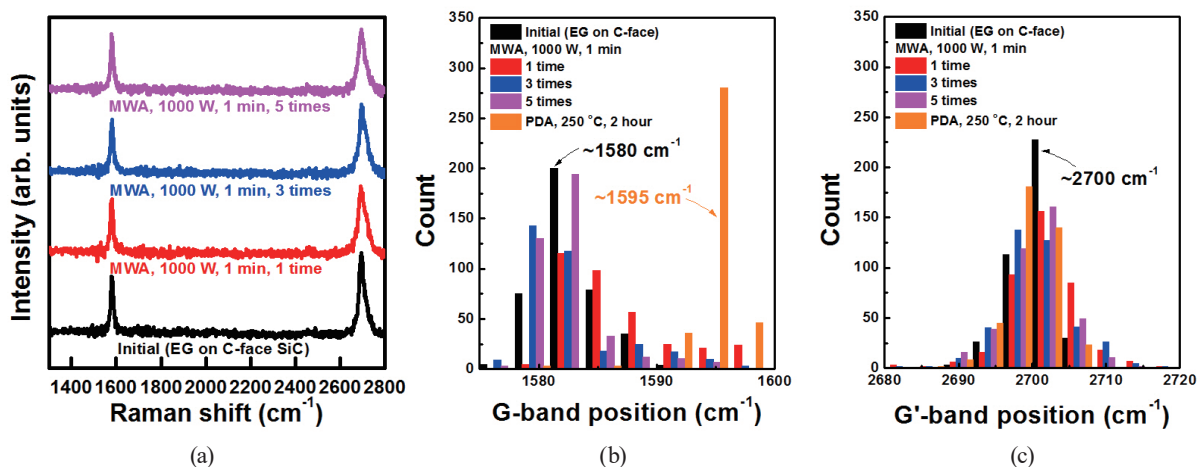


Fig. 2. (Color online) (a) Raman scattering spectra of EG after MWA, and histograms of the (b) G- and (c) G'-band positions of Raman scattering spectroscopy under various annealing conditions after the formation of the sol-Al<sub>2</sub>O<sub>3</sub> layer. One data point corresponds to one pixel ( $0.2 \times 0.2\text{ }\mu\text{m}^2$ ) in micro-Raman mapping.

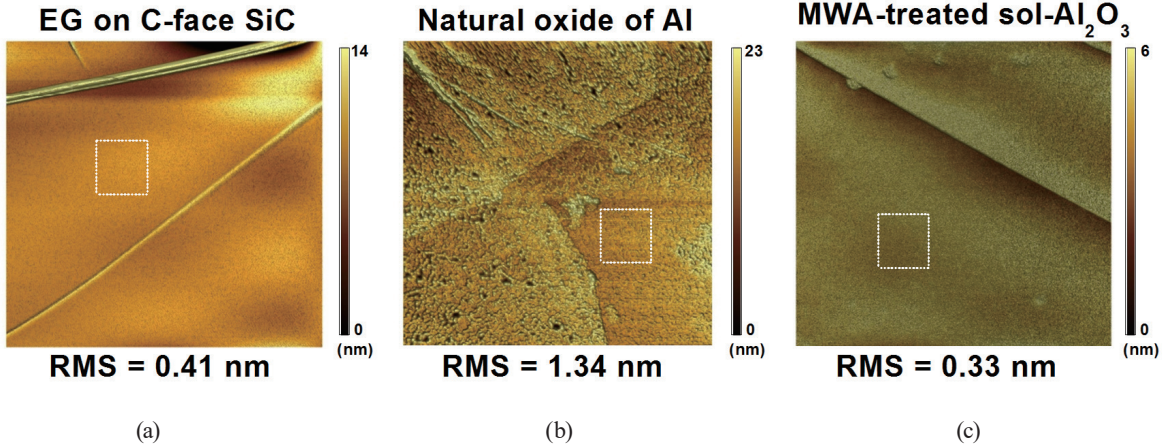


Fig. 3. (Color online) AFM images of the samples after the formation of (a) EG on C-face SiC, (b) the natural oxide layer of Al, and (c) the sol-Al<sub>2</sub>O<sub>3</sub> layer after iterations of 1 min MWA at 1000 W for 5 times. The RMS values were extracted from the area within the white square in each image.

1000 W for 5 times. The EG grown on C-face SiC shows graphene's pleatlike characteristics [Fig. 3(a)]. After the formation of a natural oxide of the Al layer, the surface consists of graphene's pleats as well as of Al clusters, giving an average RMS surface roughness as large as 1.34 nm [Fig. 3(b)]. This rugged surface morphology is a major cause of the degradation of EG-FET performance. The solution-processed Al<sub>2</sub>O<sub>3</sub> samples, on the other hand, show a flat surface morphology without Al clusters. The RMS surface roughness of the MWA-treated sol-Al<sub>2</sub>O<sub>3</sub> [Fig. 3(c)] sample was significantly reduced to 0.33 nm. This minimized surface roughness of the MWA-treated sol-Al<sub>2</sub>O<sub>3</sub> layer is ideal for fabricating high-performance EG-FETs.

### 3.3 XPS analysis of MWA-treated sol-Al<sub>2</sub>O<sub>3</sub>

To evaluate the chemical composition of the Al<sub>2</sub>O<sub>3</sub> films, we conducted an XPS analysis. Figure 4 shows the O1s and Al2p peaks of the natural oxide of Al, the sol-Al<sub>2</sub>O<sub>3</sub> fabricated with PDA, and the sol-Al<sub>2</sub>O<sub>3</sub> fabricated with MWA. The O1s peak can be deconvoluted into three Gaussian components. The component with a low binding energy (M-O<sub>Low</sub>) at ~530 eV originates from the oxygen atoms fully oxidizing the Al atoms. The second component (M-O<sub>Middle</sub>) centered at ~532 eV is attributed to the oxygen atoms in the Al<sub>2</sub>O<sub>3</sub> lattice accompanied by oxygen vacancies. The high-binding-energy component (M-O<sub>High</sub>) above 534 eV is associated with the oxygen atoms next to C- and H-bearing fragments.<sup>(20,21)</sup> A large portion of the oxygen-vacancy-related M-O<sub>Middle</sub> peak in the O1s spectrum, as well as the additional Al metal peak in the Al2p spectrum of the natural oxide of the Al sample, indicates that the predeposited Al layer is not fully oxidized just after the deposition. In sharp contrast, the PDA-treated sol-Al<sub>2</sub>O<sub>3</sub> has a single Al2p peak at ~75 eV, suggesting the formation of a more fully oxidized film. This film, however, still preserves the O<sub>high</sub> peak in O1s with a very high intensity and a wide energy

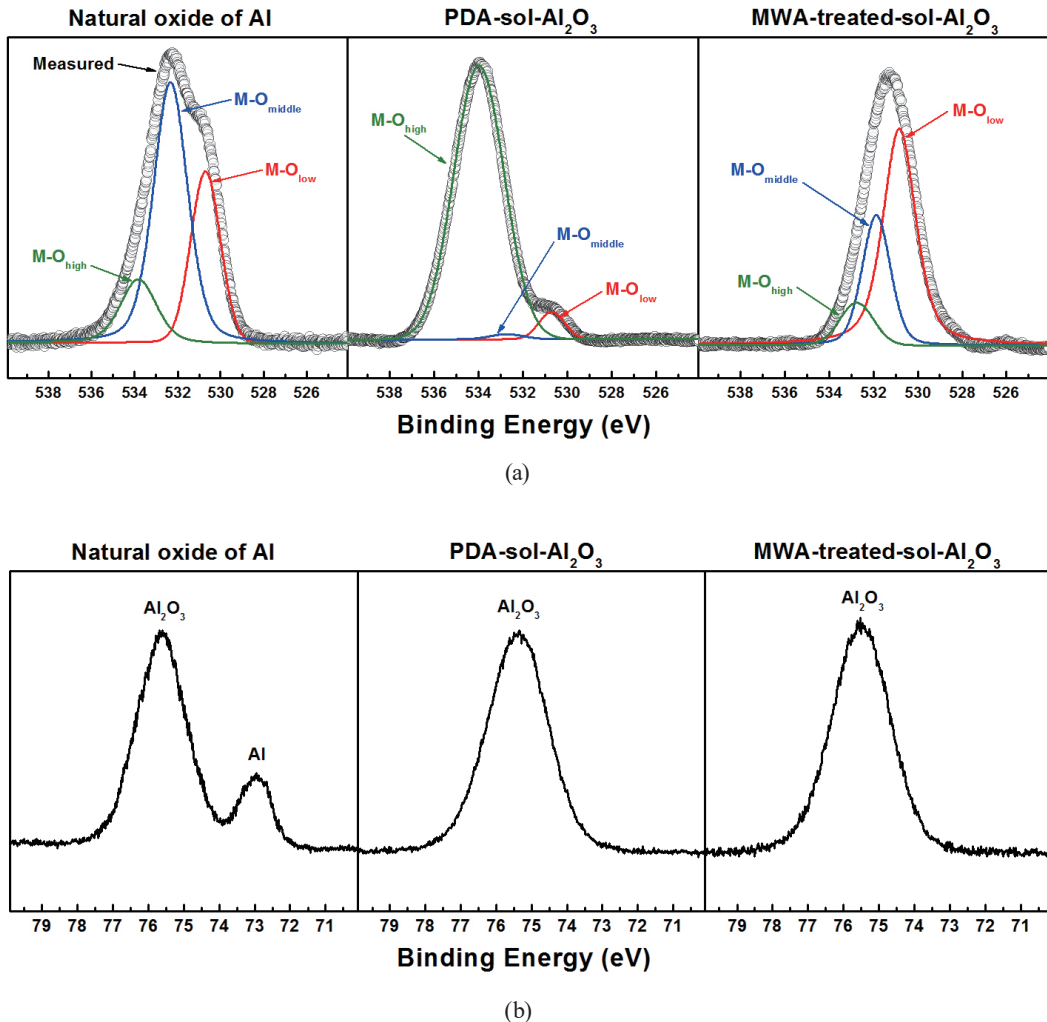


Fig. 4. (Color online) XPS spectra of (a) O1s and (b) Al2p peaks after the formation of the natural oxide layer of Al and the sol- $\text{Al}_2\text{O}_3$  layer with PDA at 250 °C for 2 h, and the sol- $\text{Al}_2\text{O}_3$  layer after iterations of 1 min MWA at 1000 W for 5 times.

distribution. Since this peak is associated with the presence of loosely bound oxygen ligands, such as  $-\text{CO}_3$ ,  $\text{H}_2\text{O}$ , and  $\text{O}_2$  molecules on the surface of the  $\text{Al}_2\text{O}_3$  film,<sup>(22)</sup> PDA is shown to be insufficient in fully eliminating such residual fragments. The MWA-treated  $\text{Al}_2\text{O}_3$ , on the other hand, can greatly reduce the M-O<sub>High</sub> peak within only 5 min of treatment. This indicates that MWA can effectively eliminate the residual C- and H-bearing fragments.

### 3.4 Electrical characteristics of MWA-treated sol- $\text{Al}_2\text{O}_3$

To evaluate the electrical properties of the sol- $\text{Al}_2\text{O}_3$  layers, we measured the leakage current density versus the electric field [Fig. 5(a)] and the capacitance–voltage characteristics [Figs.

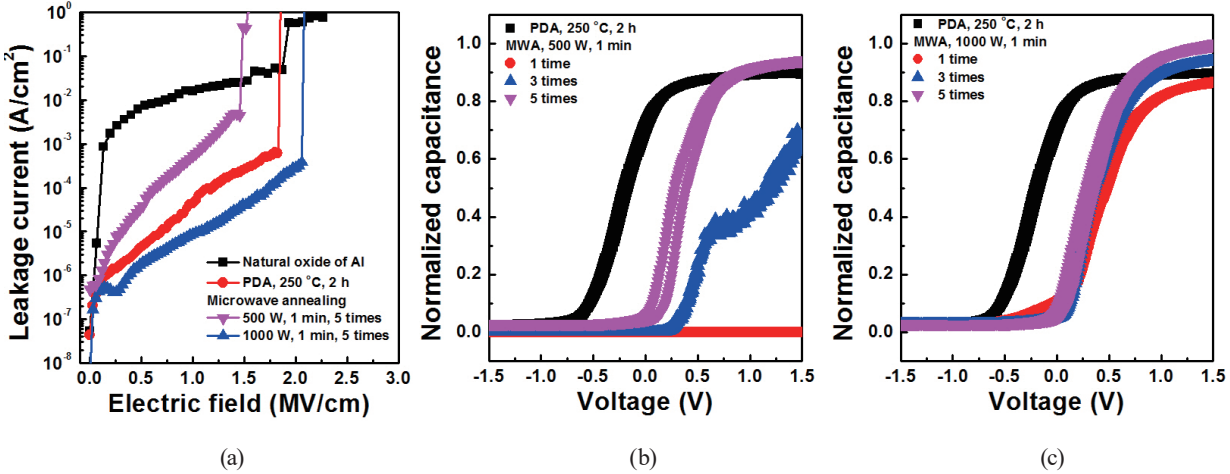


Fig. 5. (Color online) PDA- and MWA-treated  $\text{Al}_2\text{O}_3$  films. (a) Leakage current characteristics, and capacitance-voltage characteristics under the MWA condition at (b) 500 and (c) 1000 W.

5(b) and 5(c)]. The natural oxide of the Al layer shows a high leakage current density of  $1.6 \times 10^{-2} \text{ A}/\text{cm}^2$  at 1 MV/cm. It is, however, significantly reduced to  $4.29 \times 10^{-5} \text{ A}/\text{cm}^2$  in PDA-treated  $\text{Al}_2\text{O}_3$  or further to  $1.0 \times 10^{-5} \text{ A}/\text{cm}^2$  in MWA-treated  $\text{Al}_2\text{O}_3$ . This improvement is due to the formation of high-quality  $\text{Al}_2\text{O}_3$  layers by the solution process, as well as the effective elimination of the residual C- and H-bearing fragments by MWA. Figures 4(b) and 4(c) show the  $C$ - $V$  curve after MWA at 500 and 1000 W, respectively. The time evolution of the dielectric constant, a good measure of the quality of the sol- $\text{Al}_2\text{O}_3$  layer, is also shown in Table 1. The dielectric constants of the natural oxide ( $\sim 3 \text{ nm}$ ) and PDA-treated sol- $\text{Al}_2\text{O}_3$  ( $\sim 10 \text{ nm}$ ) layers are around 5.34 and 6.35, respectively. These values are too small to be applied to gate dielectrics for practical EG-FETs. The MWA-treated sol- $\text{Al}_2\text{O}_3$  layer, on the other hand, shows a dielectric constant as high as  $\sim 7.53$  (1000 W, 1 min, 5 times). For the MWA at 500 W, improvements in the capacitance and the dielectric constant are mediocre. This behavior represents the process by which an unstable sol- $\text{Al}_2\text{O}_3$  film changes into a high-quality one upon applying MWA. The capacitance and the dielectric constant under 1000 W microwave exposure saturate in only  $\sim 1$  min. These excellent properties of the MWA-treated sol- $\text{Al}_2\text{O}_3$  are ascribed to the volumetric self-heating of MWA, which minimizes the heat loss during the process. As a result, we conclude that MWA is very effective for the formation of a high-quality sol- $\text{Al}_2\text{O}_3$  layer on EG.

### 3.5 Electrical characteristics of EG-FETs with MWA-treated sol- $\text{Al}_2\text{O}_3$

Figure 6 shows the drain current and transconductance as functions of the gate voltage for the EG-FETs with (a) natural oxide of Al and (b) MWA-treated sol- $\text{Al}_2\text{O}_3$ . Table 2 shows the electrical characteristics of both devices obtained from the figure. The EG-FET with the natural oxide of Al shows a p-type ambipolar conduction behavior with the Dirac voltage ( $V_{\text{Dirac}}$ )

Table 1

Dielectric constants of samples treated under various annealing conditions.

Oxi-Al	PDA-treated sol-Al <sub>2</sub> O <sub>3</sub>	1 min MWA-treated sol-Al <sub>2</sub> O <sub>3</sub>						
		500 W 1 time	500 W 3 times	500 W 5 times	1000 W 1 time	1000 W 3 times	1000 W 5 times	
Dielectric constant	5.34	6.35	0.003	3.19	7.07	6.48	7.02	7.53

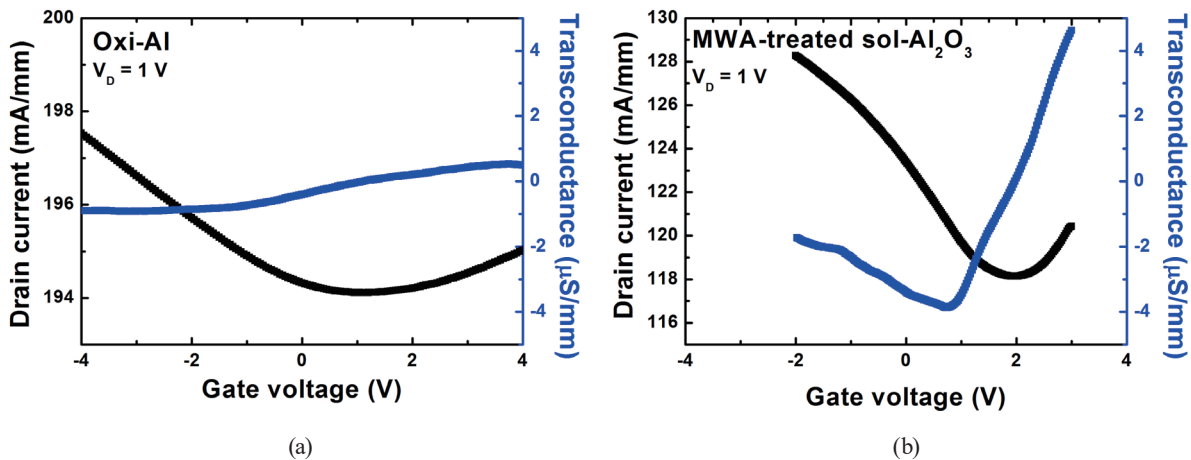
Fig. 6. (Color online) Drain current and transconductance characteristics of (a) EG-FET with natural oxide of Al and (b) EG-FET with MWA-treated sol-Al<sub>2</sub>O<sub>3</sub>.

Table 2

Electrical characteristics EG-FET with the natural oxide of Al and MWA-treated sol-Al<sub>2</sub>O<sub>3</sub>.

$V_{Dirac}$ (V)	$I_{gate}$ (nA)	SS (V/dec)	$g_m$ ( $\mu\text{S}/\text{mm}$ )		$\mu_{FE}$ ( $\text{cm}^2/\text{Vs}$ )	
			Electron	Hole	Electron	Hole
Oxi-Al <sub>2</sub> O <sub>3</sub>	1.1	0.03	587	0.4	0.9	1.2
MWA-treated sol-Al <sub>2</sub> O <sub>3</sub>	1.95	0.4	71	4.3	3.8	9.7

of 1.1 V. For the EG-FET with MWA-treated sol-Al<sub>2</sub>O<sub>3</sub>, on the other hand,  $V_{Dirac}$  is slightly shifted toward a higher voltage of 1.95 V. This suggests that the EG after the formation of the MWA-treated sol-Al<sub>2</sub>O<sub>3</sub> becomes slightly p-type-doped mostly owing to the oxygen doping. Generally, oxygen doping increases the impurity scattering, which causes the degradation of transconductance.<sup>(20)</sup> The hole transconductance ( $g_m$ ) of the EG-FET with MWA-treated sol-Al<sub>2</sub>O<sub>3</sub>, however, increased from 0.9 to 3.8  $\mu\text{S}/\text{mm}$ . The field-effect mobility also increased by a factor of 8 from that of the EG-FET with the natural oxide of Al. The subthreshold swing (SS) also significantly decreased from 587 to 71 V/dec, which suggests the improvement of the interface state between the graphene and the gate oxide.<sup>(24)</sup> The reason why these transport properties were not greatly affected by oxygen doping is open to future studies. Despite these

improvements, the field-effect mobility itself is not as high as previously reported values.<sup>(25)</sup> This degradation can be attributed to the large access length as well as to the non-optimized fabrication processes. Further improvements can be expected by optimizing the device fabrication process such as the self-align process and the preparation of a high-quality solution.

#### 4. Conclusions

We demonstrated that the formation of a damage-free, high-quality Al<sub>2</sub>O<sub>3</sub> dielectric layer is possible on EG by using a solution-based coating combined with MWA. The heavy hole doping observed in the conventional PDA-based sol-Al<sub>2</sub>O<sub>3</sub> is due to the substantial number of oxygen molecules absorbed from air. Although the process temperature of MWA was estimated to be as high as ~500 °C, the unique heating mechanism of MWA allowed the pristine properties of graphene to be retained after the process. Furthermore, the dielectric properties, such as the surface roughness, chemical stoichiometry, and electrical performance, were all improved in the proposed MWA-treated sol-Al<sub>2</sub>O<sub>3</sub>. As a result, the transconductance and field-effect mobility characteristics were remarkably improved by about 8 times compared with those of EG-FET with a natural oxide of Al. Therefore, we believe that these results provide important insights for the betterment of EG-FET-based sensor applications.

#### Acknowledgments

This work was supported by JSPS Grant-in-Aid for JSPS fellows (JP17J04947).

#### References

- 1 C. Berger, Z. Song, X. Li, X. Wu, N. Brown, C. Naud, D. Mayou, T. Li, J. Hass, A. N. Marchenkov, E. H. Conrad, P. N. First, and W. A. de Heer: *Science* **312** (2006) 1191. <http://doi.org/10.1126/science.1125925>
- 2 T. Ohta, A. Bostwick, J. L. McChesney, Th. Seyller, K. Horn, and E. Rotenberg: *Phys. Rev. Lett.* **98** (2007) 206802. <https://doi.org/10.1103/PhysRevLett.98.206802>
- 3 K. V. Emtsev, A. Bostwick, K. Horn, J. Jobst, G. L. Kellogg, L. Ley, J. L. McChesney, T. Ohta, S. A. Reshanov, J. Röhrl, E. Rotenberg, A. K. Schmid, D. Waldmann, H. B. Weber, and T. Seyller: *Nat. Mater.* **8** (2009) 203. <https://doi.org/10.1038/nmat2382>
- 4 P. Bergveld: *IEEE Trans. Biomed. Eng.* **BME-19** (1972) 342. <https://doi.org/10.1109/TBME.1972.324137>
- 5 P. Bergveld: *Sens. Actuators, B* **88** (2003) 1. [https://doi.org/10.1016/S0925-4005\(02\)00301-5](https://doi.org/10.1016/S0925-4005(02)00301-5)
- 6 B. Lee, S. Y. Park, H. C. Kim, K. J. Cho, E. M. Vogel, M. J. Kim, R. M. Wallace, and J. Kim: *Appl. Phys. Lett.* **92** (2008) 203102. <https://doi.org/10.1063/1.2928228>
- 7 X. Lu, H. Huang, N. Nemchuk, and R. S. Ruoff: *Appl. Phys. Lett.* **75** (1999) 193. <https://doi.org/10.1063/1.124316>
- 8 J. E. Lee, G. Ahn, J. Shim, Y. S. Lee, and S. Ryu: *Nat. Commun.* **3** (2012) 1024. <https://doi.org/10.1038/ncomms2022>
- 9 A. R. Phani and S. Santucci: *J. Non-Cryst. Solids* **352** (2006) 4093. <https://doi.org/10.1016/j.jnoncrysol.2006.06.013>
- 10 R. Luque, J. A. Menendez, A. Arenillas, and J. Cot: *Energy Environ. Sci.* **5** (2012) 5481. <https://doi.org/10.1039/C1EE02450G>
- 11 K. K. Banger, Y. Yamashita, K. Mori, R. L. Peterson, T. Leedham, J. Rickard, and H. Sirringhaus: *Nat. Mater.* **10** (2011) 45. <https://doi.org/10.1038/nmat2914>
- 12 S. Y. Han, G. S. Herman, and C. H. Chang: *J. Am. Chem. Soc.* **133** (2011) 5166. <https://doi.org/10.1021/ja104864j>

- 13 P. K. Nayak, M. N. Hedhili, D. Cha, and H. N. Alshareef: *Appl. Phys. Lett.* **100** (2012) 202106. <https://doi.org/10.1063/1.4718022>
- 14 D. Michael, P. Mingos, and D. R. Baghurst: *Chem. Soc. Rev.* **20** (1991) 1. <https://doi.org/10.1039/CS9912000001>
- 15 A. M. Surati, S. Jauhari, and K. R. Desai: *Arch. Appl. Sci. Res.* **4** (2012) 645.
- 16 J. H. Chen, M. Liu, T. Yang, F. M. Zhai, X. M. Hou, and K. C. Chou: *CrystEngComm* **19** (2017) 519. <https://doi.org/10.1039/c6ce02285e>
- 17 S. G. Sundaresan, M. Rao, Y. Tian, M. C. Ridgway, J. A. Schreibels, and J. J. Kopanski: *J. Appl. Phys.* **101** (2007) 073708. <https://doi.org/10.1063/1.2717016>
- 18 A. Das, S. Pisana, S. Piscanec, B. Chakraborty, S. K. Saha, U. V. Waghmare, R. Yang, H. R. Krishnamurthy, A. K. Geim, A. C. Ferrari, and A. K. Sood: *Nat. Nanotechnol.* **3** (2008) 210. <https://doi.org/10.1038/nnano.2008.67>
- 19 J. M. Kremsner and C. O. Kappe: *J. Org. Chem.* **71** (2006) 4651. <https://doi.org/10.1021/jo060692v>
- 20 M. R. Alexander, G. E. Thompson, X. Zhou, G. Beamson, and N. Fairley: *Surf. Interface Anal.* **34** (2002) 485. <https://doi.org/10.1002/sia.1344>
- 21 L. Wang, T. Shinohara, and B. P. Zhang: *Appl. Surf. Sci.* **256** (2010) 5807. <https://doi.org/10.1016/j.apsusc.2010.02.058>
- 22 H. Tong, Z. Deng, Z. Liu, C. Huang, J. Huang, H. Lana, C. Wang, and Y. Cao: *Appl. Surf. Sci.* **257** (2011) 4906. <https://doi.org/10.1016/j.apsusc.2010.12.144>
- 23 J. H. Chen, C. Jang, S. Adam, M. S. Fuhrer, E. D. Williams, and M. Ishigami: *Nat. Phys.* **4** (2008) 377. <https://doi.org/10.1038/nphys935>
- 24 J. Zhu, R. Jhaveri, and J. C. S. Woo: *Appl. Phys. Lett.* **96** (2010) 193503. <https://doi.org/10.1063/1.3428785>
- 25 Y. M. Lin, C. Dimitrakopoulos, K. A. Jenkins, D. B. Farmer, H. Y. Chiu, A. Grill, and Ph. Avouris: *Science* **327** (2010) 662. <https://doi.org/10.1126/science.1184289>

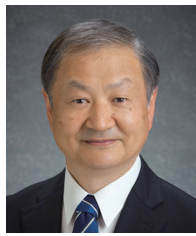
## About the Authors



**Kwan-Soo Kim** received his B.S. and M.S. degrees in electronic materials engineering from Kwangwoon University, Seoul, Korea in 2007 and 2009, respectively, and his Ph.D. degree in electronic engineering from Tohoku University, Sendai, Japan, in 2014. From 2009 to 2014, he worked for the Electronics and Telecommunications Research Institute (ETRI), Daejeon, Korea, where he conducted research on biosensors using photodetectors. He is currently a postdoctoral researcher at the Research Institute of Electrical Communication (RIEC), Tohoku University. His current research interests include graphene-based nanoelectronic devices and their applications. (kimks@riec.tohoku.ac.jp)



**Hirokazu Fukidome** received his B.Eng., M.Eng., and Ph.D. degrees from Osaka University, Osaka, Japan, in 1995, 1997, and 2000, respectively. He was a Postdoctoral Fellow at Bell Telephone Laboratories from 2000 to 2001, and then at RIKEN from 2001 to 2002. From 2002 to 2007, he was an assistant professor at Toyota Technological Institute. Since 2008, he has been with Tohoku University, Sendai, Japan. Since 2012, he has been an associate professor at the Research Institute of Electrical Communication (RIEC), Tohoku University. His research interest is in semiconductor nanofabrication and nanodevice applications, spectromicroscopy for the operando analysis of nanodevices, and surface electrochemistry. Dr. Fukidome is a member of the Japanese Society of Applied Physics, the Surface Science Society of Japan, and the Electrochemical Society of Japan. (fukidome@riec.tohoku.ac.jp)



**Maki Suemitsu** received his B.Eng., M.Eng., and Ph.D. degrees in electronic engineering from Tohoku University, Sendai, Japan, in 1975, 1977, and 1980, respectively. He worked as a research associate from 1980 to 1989, and then as an associate professor from 1990 to 2002 at the Research Institute of Electrical Communication (RIEC), Tohoku University. In 2003, he joined the Center for Interdisciplinary Research, Tohoku University, as a professor, and has been a professor at RIEC since 2008. His research interests include the epitaxy of group-IV materials on Si substrates and its use in devices, which are currently converging in graphene-on-silicon technology. He is the author of more than 200 papers. Professor Suemitsu is the recipient of the 30th Kumagai Award of the Vacuum Society of Japan. He is a member of the Japan Society of Applied Physics, the Vacuum Society of Japan, the Electrochemical Society, and the Materials Research Society.

(suemitsu@riec.tohoku.ac.jp)